Preprints of the 2012 20th Mediterranean Conference on Control & Automation (MED), Barcelona, Spain, July 3-6, 2012

GRADIENT METHOD OPTIMIZATION OF PENICILLIN PRODUCTION: NEW STRATEGIES

Matej Pčolka *
Faculty of Electrical Engineering
Czech Technical University in Prague
Prague, Czech Republic
email: pcolkmat@fel.cvut.cz

Sergej Čelikovský †
Institute of Information Theory and Automation
Academy of Sciences of the Czech Republic
Prague, Czech Republic
email: celikovs@utia.cas.cz

Abstract
Since their discovery, fermentation processes have gone along not only with the industrial beverages production and breweries but since the times of Alexander Fleming they have become a crucial part of the health care due to antibiotics production (from which the overwhelming majority of 90% is produced during a fermentation process). However, complicated dynamics and strong nonlinearities cause that the production with the use of linear control methods achieves only suboptimal yields. From the variety of nonlinear approaches, gradient method has proved the ability to handle these issues - nevertheless, its potential in the field of fermentation processes has not been revealed completely. In this paper, two fresh control strategies are introduced and compared - both of them are based on a double-input optimization approach, yet a successful reduction to a single-input optimization task is proposed. To accomplish this, model structure used in the previous work has been modified so that it corresponds with the new optimization strategies which together with the model stands for the main contribution of this paper.

Key words
Fermentation process, penicillin, gradient method, optimization

1 Introduction

Rapid increase of the industrial productivity of antibiotics that might be witnessed during the last few decades is basically owed to a massive improvement of production technologies rather than to sophisticated control background. As a consequence, only suboptimal operation manners have been involved with final product concentrations deep below maximum reachable values. The important next step is to consider and carefully analyze all advantages and disadvantages of the used control strategy. A wide variety of ways how to operate the input feed flow (which influences the formation of the final product especially by the amount of the substrate nutrient supplied to system through it) has been discussed in literature so far. As an initial attempt, one can consider indirect feedback methods for nutrient feeding based on pH or dissolved oxygen measurements [1] - the substrate concentration is then maintained at predetermined setpoint by either a simple open loop controller [2] or an on/off [3] or a PID type controller, followed by fuzzy approaches which appeared in the 1990s [4] and have been revitalized at the beginning of the millennium [5]. However, the most impressive results have been reached using model predictive control (MPC) approach [6]. The main drawback of this method is the fact that it is usually performed either with an approximately or exactly linearized mathematical model of the controlled process. Approximate linearization performed at certain operating point can be invalid for operating points far away from the original one (and it is known that the operating points range varies a lot during the cultivation) and each-step approximate linearization can be prohibitively time consuming. Moreover, no stability assumptions can be made for the approximate models obtained at each step and even one unstable model obtained by approximate linearization can degrade the MPC performance vastly. Exact linearization blows all these problems away - unfortunately, in the area of fermentation processes, the existence of exact linearization is rather rare and occasional. Therefore, a proper alternative is needed - gradient descent method which has already proved encouraging results in various research areas [7], [8], [9] is a strong candidate as it can handle even a nonlinear process model very effectively. The crucial point for this model based method is the availability of a mathematical model describing the biochemical process and determining an adequate cost functional to be optimized. The aim of this paper is to continue previous efforts of authors in [10] where they considered the simplified model structure reducing number of relevant inputs. The current paper considers two inputs instead of one and presents two approaches how to use such an extra freedom. To keep simplicity of the optimization task, correspondingly two alternative methods how to reduce double input problem into a single input one are presented. Such an approach results into enhanced optimization strategies giving promising outcome suitable for use in industrial practice.

The paper is organized as follows: Section 2 introduces nonlinear dynamical model of the fermentation process which is used for the optimization purposes. The penicillin cultivation is chosen to represent the fermentation processes, modification of the previously used model (which is crucial for the use of new control strategy introduced later in this paper) is explained. In Section 3, the optimization issues of the final product concentration maximization including the constraints specification are formulated. The gradient method is introduced, its theoretical background is clarified and having done the necessary problem order reduction, fresh control strategies are proposed. In Section 4, results of constant volume strategy and constant vaporization strategy are presented, compared to those obtained using strategy presented earlier and discussed. Section 5 concludes the paper.

2 Model of the fermentation process

Let us consider a penicillin cultivation [10], [11], [6] described by the following model:

$$\begin{aligned}
\frac{\mathrm{d}V}{\mathrm{d}t} &= u - V\lambda(e^{w\frac{T_{oper}-T_f}{T_b-T_f}} - 1),\\
\frac{\mathrm{d}C_X}{\mathrm{d}t} &= (\mu - K_D)C_X - \frac{\mathrm{d}V}{\mathrm{d}t}\frac{C_X}{V},\\
\frac{\mathrm{d}C_S}{\mathrm{d}t} &= -\sigma C_X + \frac{C_{S,in}u}{V} - \frac{\mathrm{d}V}{\mathrm{d}t}\frac{C_S}{V},\\
\frac{\mathrm{d}C_P}{\mathrm{d}t} &= \pi C_X - K_H C_P - \frac{\mathrm{d}V}{\mathrm{d}t}\frac{C_P}{V}.
\end{aligned} \tag{1}$$

*The work of M. Pčolka was supported by internal Grant of the Czech Technical University no 161-802830/13135.

†The work of S. Čelikovský was supported by the Czech Science Foundation through the research grant no. P103/12/1794.

Here $V\,(\mathrm{l})$ refers to cultivation broth volume, $C_X\,(\mathrm{gl}^{-1})$ represents biomass concentration, $C_S\,(\mathrm{gl}^{-1})$ stands for the limiting substrate concentration (let us consider carbon to be the limiting substrate) and $C_P\,(\mathrm{gl}^{-1})$ represents the final product (penicillin) concentration. The substrate feed flow rate $u\,(\mathrm{lh}^{-1})$ is considered to be the operated input to the model.

Parameters $\lambda\,(\mathrm{h}^{-1})$, and $w\,(-)$ are specific vaporization constants, $T_{oper}\,(\mathrm{K})$ represents empirically obtained operational temperature $T_{opt}\,(\mathrm{K})$ [12], and $T_f\,(\mathrm{K})$ and $T_b\,(\mathrm{K})$ refer to the freezing temperature and the boiling temperature of the broth, respectively, which are considered to be the same as those of the water [6].

A simple constant term $K_D\,(\mathrm{h}^{-1})$ models biomass death kinetics while the total of specific biomass growth rate $\mu\,(\mathrm{h}^{-1})$ and the specific production rate $\pi\,(\mathrm{gg_{DW}}^{-1}\mathrm{h}^{-1})$ weighted by biomass on substrate yield coefficient $Y_{X/S}$ and the product on substrate yield coefficient $Y_{P/S}$ gives specific substrate consumption rate $\sigma\,(\mathrm{gg_{DW}}^{-1}\mathrm{h}^{-1}) = Y_{X/S}^{-1}\mu + Y_{P/S}^{-1}\pi$. In this paper, Contois kinetics of the biomass growth [13] and Haldane kinetics [14] of the product formation are considered, which results in the following expressions for the μ and π:

$$\begin{aligned}\mu &= \mu_{max}\frac{C_S}{K_X C_X + C_S},\\ \pi &= \pi_{max}\frac{C_S}{K_P + C_S + C_S^2/K_I},\end{aligned} \tag{2}$$

where $\mu_{max}\,(\mathrm{gg_{DW}}^{-1}\mathrm{h}^{-1})$, $\pi_{max}\,(\mathrm{gg_{DW}}^{-1}\mathrm{h}^{-1})$ are the maximum specific growth and production rates, $K_X\,(\mathrm{gg_{DW}}^{-1})$ is the Contois saturation constant, $K_P\,(\mathrm{gl}^{-1})$ is product formation saturation constant and $K_I\,(\mathrm{gl}^{-1})$ is product formation inhibition constant for product formation.

Input substrate concentration $C_{S,in}\,(\mathrm{gl}^{-1})$ reflects the effect of the input flow u on the substrate concentration C_S. Finally, penicillin hydrolysis is modeled by a degradation constant $K_H\,(\mathrm{h}^{-1})$. At this point, more interested readers are referred to [11] and [6] where the model is described in more details.

Now, let us assume, that the cultivation volume V can not only be increased by exogenous input u, but a volume withdrawal can be performed as well. This requires a new input variable to be introduced and the volume differential equation changes into:

$$\frac{\mathrm{d}V}{\mathrm{dt}} = u_1 - V\lambda(e^{w\frac{T_{oper}-T_f}{T_b-T_f}} - 1) - u_2, \tag{3}$$

where u_1 corresponds with the old input variable and $u_2\,(\mathrm{lh}^{-1})$ stands for volume withdrawal.

This little change of volume differential, however, effects the differential equations of other state variables as well. Let us remind that the state variables are in form of concentration which cannot be increased nor decreased by volume withdrawal. Therefore, terms including volume differential should be modified as follows: $\mathrm{d}V/\mathrm{dt} \to \mathrm{d}V/\mathrm{dt} + u_2$.

For the needs of optimization and in order to follow the conventional notation, let us rewrite the enhanced model 1 into the ordinary form using $x^{\mathrm{T}} = [V, C_X, C_S, C_P]$ and $u^{\mathrm{T}} = [u_1, u_2]$:

$$\begin{aligned}
\dot{x}_1 &= u_1 - \lambda(e^{w\frac{T_{oper}-T_f}{T_b-T_f}} - 1)x_1 - u_2,\\
\dot{x}_2 &= \left(\mu_{max}\frac{x_3}{K_X x_2 + x_3} - K_D\right)x_2 - \left(u_1 - \lambda\left(e^{w\frac{T_{oper}-T_f}{T_b-T_f}} - 1\right)x_1\right)\frac{x_2}{x_1},\\
\dot{x}_3 &= -\left(\frac{\mu_{max}}{Y_{X/S}}\frac{x_3}{K_X x_2 + x_3} + \frac{\pi_{max}}{Y_{P/S}}\frac{x_3}{K_P + x_3 + x_3^2/K_I}\right)x_2 + \frac{C_{S,in}u_1}{x_1} - \left(u_1 - \lambda\left(e^{w\frac{T_{oper}-T_f}{T_b-T_f}} - 1\right)x_1\right)\frac{x_3}{x_1},\\
\dot{x}_4 &= \pi_{max}\frac{x_3}{K_P + x_3 + x_3^2/K_I}x_2 - K_H x_4 - \left(u_1 - \lambda\left(e^{w\frac{T_{oper}-T_f}{T_b-T_f}} - 1\right)x_1\right)\frac{x_4}{x_1}.
\end{aligned} \tag{4}$$

3 Optimal control design

In [10], an optimal feeding strategy coming out of a gradient projection method has been introduced. Theoretical complication given by the state dependence of the input saturation has been successfully addressed and assumption on sufficiently large cultivation tank volume has been made. However, in industrial application, the cultivation tank may be filled up with a such large initial volume that applying computed input feed flow rate leads to tank overflow in short horizon. A perspective offering solution to this problem has been tackled in the previous section. Here, we propose two new control strategies operating the second input and bringing interesting results improvement.

3.1 A constant volume strategy

By applying another exogenous input u_2, one can avoid tank overflow, yet another problem occurs. A thoroughful reader has surely already noticed that having introduced two input variables, the first differential equation of mathematical description of the system does not comply with physical laws. It can be shown that at certain finite time point the volume can reach zero value and further withdrawal can theoretically cause negative volume, which is physically impossible. One way of avoiding this is to set a dynamical constraint on the second input u_2 which ensures that at the point of zero volume V the withdrawal does not exceed the inlet flow. However, looking at the issue from the engineering point of view, it is not either convenient to decrease the volume below certain too low value as the final product amount equals to product concentration C_P multiplied by the volume V.

Let us introduce an idea leading to a strategy solving the sketched negative volume difficulty. It consists in an assumption that the second input u_2 is used to compensate the effect of the first input u_1 on the volume V. In other words, we require the second input to be able to hold the volume constant - from the first differential equation of the model 4 which should be equal to zero, the second input u_2

can be calculated directly as $u_2 = u_1 - K_{vap}V_0$, where V_0 is the initial state and K_{vap} is the overall vaporization constant, $K_{vap} = \lambda \exp(w\frac{T_{oper}-T_f}{T_b-T_f} - 1)$. As the first differential equation is identically equal to zero and the second input u_2 effects only the first state equation, the system gets simplified into the following three-state model with state variables $\xi^{\mathrm{T}} = [C_X, C_S, C_P]$ and one optimization variable υ corresponding with u_1 in model 4:

$$\begin{aligned}
\dot{\xi}_1 &= \left(\mu_{max}\frac{\xi_2}{K_X\xi_1+\xi_2} - K_D\right)\xi_1 - (\upsilon - K_{vap}V_0)\,\frac{\xi_1}{V_0},\\
\dot{\xi}_2 &= -\left(\frac{\mu_{max}}{Y_{X/S}}\frac{\xi_2}{K_X\xi_1+\xi_2} + \frac{\pi_{max}}{Y_{P/S}}\frac{\xi_2}{K_P+\xi_2+\xi_2^2/K_I}\right)\xi_1 + \frac{C_{S,in}\upsilon}{V_0} - (\upsilon - K_{vap}V_0)\,\frac{\xi_2}{V_0},\\
\dot{\xi}_3 &= \pi_{max}\frac{\xi_2}{K_P+\xi_2+\xi_2^2/K_I}\xi_1 - K_H\xi_3 - (\upsilon - K_{vap}V_0)\,\frac{\xi_3}{V_0}.
\end{aligned} \tag{5}$$

Model 5 supplemented by the corresponding model parameters (Tab. 1) provides an engineer with a tool to design the optimal control minimizing a properly chosen criterion. Let us remark that V_0 is a parameter that can be specified individually.

Table 1. Model parameters.

Parameter	Value	Parameter	Value
μ_{max}	0.11	$Y_{P/S}$	1.2
π_{max}	0.004	$C_{S,in}$	500
K_P	0.1	K_{vap}	6.23×10^{-4}
$Y_{X/S}$	0.47	K_I	0.1
K_D	0.0136	T_{oper}	298
K_X	0.06	T_f	273
K_H	0.01	T_b	373

3.2 A constant vaporization strategy

Although not spoken directly, the constant volume strategy requires except of input constraints yet another restricting condition - it is the fact, that the volume differential $\dot{V}$ equals to zero. Although working well, in some cases this restriction can be too conservative and liberalizing it, slightly better results can be expected.

The liberalization consists in the idea that not the volume but its relative change is required to be constant and (in order to keep the issue simple) in absolute value equal to the vaporization constant. Expressed mathematically, $\mathrm{d}V/\mathrm{dt} = -K_{vap}V$. This implies an input constraint $u_2 = u_1$ and although the optimization model returns to a more involved four-state form with $\bar{\xi} = [V, C_X, C_S, C_P]$, it still stays with the only optimization variable $\bar{\upsilon}$ (corresponding to the inlet flow u_1). Let us resume the optimized plant description (the parameter values match with those given in Tab. 1):

$$\begin{aligned}
\dot{\bar{\xi}}_1 &= -K_{vap}\bar{\xi}_1,\\
\dot{\bar{\xi}}_2 &= \left(\mu_{max}\frac{\bar{\xi}_3}{K_X\bar{\xi}_2+\bar{\xi}_3} - K_D\right)\bar{\xi}_2 - \left(\bar{\upsilon} - K_{vap}\bar{\xi}_1\right)\frac{\bar{\xi}_2}{\bar{\xi}_1},\\
\dot{\bar{\xi}}_3 &= -\left(\frac{\mu_{max}}{Y_{X/S}}\frac{\bar{\xi}_3}{K_X\bar{\xi}_2+\bar{\xi}_3} + \frac{\pi_{max}}{Y_{P/S}}\frac{\bar{\xi}_3}{K_P+\bar{\xi}_3+\bar{\xi}_3^2/K_I}\right)\bar{\xi}_2 + \frac{C_{S,in}\bar{\upsilon}}{\bar{\xi}_1} - \left(\bar{\upsilon} - K_{vap}\bar{\xi}_1\right)\frac{\bar{\xi}_3}{\bar{\xi}_1},\\
\dot{\bar{\xi}}_4 &= \pi_{max}\frac{\bar{\xi}_3}{K_P+\bar{\xi}_3+\bar{\xi}_3^2/K_I}\bar{\xi}_2 - K_H\bar{\xi}_4 - \left(\bar{\upsilon} - K_{vap}\bar{\xi}_1\right)\frac{\bar{\xi}_4}{\bar{\xi}_1}.
\end{aligned} \tag{6}$$

3.3 Optimization task formulation

From the optimization point of view, penicillin production optimization can be viewed as fixed initial state, free time interval and free final state issue. Without any loss of generality and due to upper cultivation duration constraint, let us now consider multiple optimization routines with fixed time intervals of length $t_{j,end} \in \{200, 300, 400, 500\}$ where j denotes certain optimization routine. This helps us to simplify the optimization procedure and avoid difficulties with general time interval solution.

For the purpose of the optimization using the two introduced strategies, the objective functionals reflecting the optimization effort needs to be formulated. As the main goal is to maximize the final product concentration, the following criteria in the Mayer form are formulated:

$$\begin{aligned}
\mathcal{J} &= -\xi_3(t_{end}),\\
\bar{\mathcal{J}} &= -\bar{\xi}_4(t_{end}),
\end{aligned} \tag{7}$$

where $\mathcal{J}$ denotes the criterion for the constant volume strategy and $\bar{\mathcal{J}}$ refers to the constant vaporization strategy criterion.

Regarding state optimization constraints, it can be shown that the new models 5 and 6 satisfy physical constraints (state variables nonnegativity) and no further attention is necessary to pay to low state constraints. Moreover, both strategies eliminate the need for upper volume constraint handling.

Thus, input saturation constraint $0 \leq \upsilon, \bar{\upsilon} \leq U_{max}$ and input piecewise constant character $\mathrm{d}\upsilon/\mathrm{dt} = 0$, $\mathrm{d}\bar{\upsilon}/\mathrm{dt} = 0$ for $ml \leq t < (m+1)l,\ m = 0, 1, \ldots$ (accomplished by sampling of the inputs υ, $\bar{\upsilon}$ with sampling period $l = 4\,\mathrm{h}$) are the only static constraints related to these optimization tasks.

Having properly defined the system equations, the input constraints and the objective functionals, the optimization problems for $t \in [t_0, t_{end}]$ (without any loss of generality, let us consider $t_0 = 0\,\mathrm{h}$) can be summarized:

$$\begin{aligned} \upsilon^*(t) &= \arg\min_{\upsilon(t)} \mathcal{J}\left(\xi(t)\right), \\ \bar{\upsilon}^*(t) &= \arg\min_{\bar{\upsilon}(t)} \bar{\mathcal{J}}\left(\bar{\xi}(t)\right) \end{aligned} \tag{8}$$

such that the following constraints hold:

$$\begin{aligned} \dot{\xi}(t) &= f(\xi(t), \upsilon(t)), \\ \dot{\bar{\xi}}(t) &= \bar{f}(\bar{\xi}(t), \bar{\upsilon}(t)), \\ \xi(t_0) &= \xi_0, \\ \bar{\xi}(t_0) &= \bar{\xi}_0, \\ 0 \leq \upsilon(t), \bar{\upsilon}(t) &\leq U_{max}. \end{aligned} \tag{9}$$

Here, $f(\xi(t), \upsilon(t))$ and $\bar{f}(\bar{\xi}(t), \bar{\upsilon}(t))$ refer to the models 5 and 6, respectively. The values of ξ_0, $\bar{\xi}_0$ and U_{max} are summarized in tab. 2.

Table 2. Optimization constraints.

Parameter	Value
$\bar{\xi}_{1,0}$	to be specified
$\xi_{1,0}$, $\bar{\xi}_{2,0}$	1.5
$\xi_{2,0}$, $\bar{\xi}_{3,0}$	6
$\xi_{3,0}$, $\bar{\xi}_{4,0}$	0
U_{max}	0.05

3.4 Nonlinear gradient method

This method belongs to family of the optimal control methods [15]. For the problems stated by 8 and the constraints given in the form of 9, the optimal inputs υ^*, $\bar{\upsilon}^*$ are searched iteratively. First of all, the initial input vectors υ_0, $\bar{\upsilon}_0$ are estimated (in our case, zero vectors have been chosen). Then, the following procedure is applied:

$$\begin{aligned} \upsilon^*_{k+1} &= \upsilon^*_k - \alpha \frac{\partial \mathcal{J}}{\partial \upsilon}, \\ \bar{\upsilon}^*_{k+1} &= \bar{\upsilon}^*_k - \alpha \frac{\partial \bar{\mathcal{J}}}{\partial \bar{\upsilon}}, \end{aligned} \tag{10}$$

where $k = 0, 1, 2, \ldots$ is the number of the iteration and α is the search step parameter. Here it should be noted that direct calculation of $\partial\mathcal{J}/\partial\upsilon$, $\partial\bar{\mathcal{J}}/\partial\bar{\upsilon}$ is quite complicated due to the fact, that ξ_3 depends on υ ($\bar{\xi}_4$ depends on $\bar{\upsilon}$) via a differential equation. Therefore, let us rather introduce Hamiltonians $\mathcal{H}$, $\bar{\mathcal{H}}$ in the following form:

$$\begin{aligned} \mathcal{H} &= p^{\mathrm{T}} f, \\ \bar{\mathcal{H}} &= \bar{p}^{\mathrm{T}} \bar{f}. \end{aligned} \tag{11}$$

Here, f, $\bar{f}$ refer to the models 5, 6 and p, $\bar{p}$ are the adjoint state vectors solved back in time. To compute the gradients of 7 with respect to $\upsilon(t)$ and $\bar{\upsilon}(t)$, set first:

$$\begin{aligned} -\dot{p} &= \frac{\partial \mathcal{H}}{\partial \xi}, \\ -\dot{\bar{p}} &= \frac{\partial \bar{\mathcal{H}}}{\partial \bar{\xi}}, \\ \dot{\xi} &= \frac{\partial \mathcal{H}}{\partial p}, \\ \dot{\bar{\xi}} &= \frac{\partial \bar{\mathcal{H}}}{\partial \bar{p}}, \\ \xi(t_0) &= \xi_0, \\ \bar{\xi}(t_0) &= \bar{\xi}_0, \\ p(t_{end}) &= -\left(\frac{\mathrm{d}\phi}{\mathrm{d}\xi}|_{t=t_{end}}\right), \\ \bar{p}(t_{end}) &= -\left(\frac{\mathrm{d}\bar{\phi}}{\mathrm{d}\bar{\xi}}|_{t=t_{end}}\right), \end{aligned} \tag{12}$$

where ϕ, $\bar{\phi}$ are the terminal terms of the optimization criteria. In our case, $\phi = -\xi_3(t_{end})$ and $\bar{\phi} = -\bar{\xi}_4(t_{end})$ from which it follows $p(t_{end}) = [0, 0, 1]^{\mathrm{T}}$, $\bar{p}(t_{end}) = [0, 0, 0, 1]^{\mathrm{T}}$. It can be shown (mathematically rigorous proof is beyond the scope of this paper) that $\partial\mathcal{J}/\partial\upsilon = -\partial\mathcal{H}/\partial\upsilon$, $\partial\bar{\mathcal{J}}/\partial\bar{\upsilon} = -\partial\bar{\mathcal{H}}/\partial\bar{\upsilon}$ and thus, gradients $\partial\mathcal{H}/\partial\upsilon$ and $\partial\bar{\mathcal{H}}/\partial\bar{\upsilon}$ can be used in iterative procedure 10, which changes into:

$$\begin{aligned} \upsilon^*_{k+1} &= \upsilon^*_k + \alpha \frac{\partial \mathcal{H}}{\partial \upsilon}, \\ \bar{\upsilon}^*_{k+1} &= \bar{\upsilon}^*_k + \alpha \frac{\partial \bar{\mathcal{H}}}{\partial \bar{\upsilon}}. \end{aligned} \tag{13}$$

Due to the overall nonconvexity of the problem, a constant search step parameter has been chosen $\alpha = 0.002$. Input saturation constraints are handled by mapping the iterated input vectors υ_{k+1} and $\bar{\upsilon}_{k+1}$ on an admissible input sets $\Upsilon_{admiss} = \{\upsilon, 0 \leq \upsilon \leq U_{max}\}$, $\bar{\Upsilon}_{admiss} = \{\bar{\upsilon}, 0 \leq \bar{\upsilon} \leq U_{max}\}$ by a simple saturation. Requirement of piecewise constant nature of the inputs υ, $\bar{\upsilon}$ is satisfied by sampling with sampling period $l = 4\,\mathrm{h}$.

The iterative procedures described by 13 terminate at the moment when negatively taken value of the decrease between the k-th and the $k+1$-st criterion value is less than a chosen tolerance.

4 Optimization results

In this section, results obtained by the proposed strategies are presented and compared to those obtained by the original one-input gradient method optimization (CG) presented in [10]. The optimization results have been simulated with the penicillin cultivation model in MATLAB environment.

4.1 Strategy results comparison

First, both the constant volume (CVol) strategy and the constant vaporization (CVap) strategy has been tested on simulations with initial volume $V_0 = 7\,\mathrm{l}$. Figure 1 shows very satisfactory cultivation results and reveals a slight superiority of the CVap strategy. It is due to the fact, that the effect of input feed flow is inversely proportional to the actual amount of broth in tank. While the effect of the input feed flow is always the same with the constant volume strategy, with the constant vaporization its positive influence improves as the volume decreases with time. Next, from the picture, it is obvious that the

cultivation period that contributes to the final product concentration $C_P(t_{end})$ the most takes approximately the last 75 h. A rapid product concentration increase can be observed during this period, however, the biomass concentration decreases badly. This has a simple biological explanation - as can be seen from the characters of both μ and π (see Eq. 2), increasing one of them, the second one decreases, which corresponds to the fact that either the biomass population growth or the penicillin production is being preferred at the very same time.

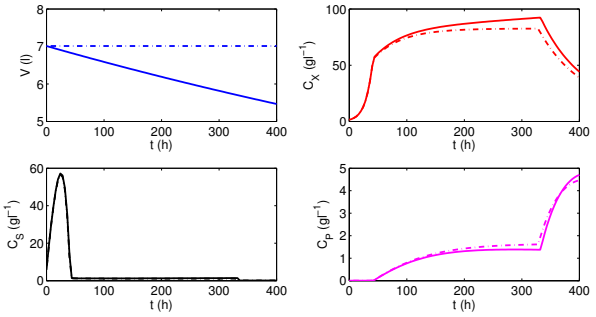

Figure 1. State profiles - comparison (CVol - dashdot, CVap - full).

4.2 Volume dependency

Next in this paper, the strategies have been tested on multiple simulations with various initial volume V_0. Initial volume conditions have been chosen as linearly increasing, $V_0(1) = 7 + 3k$, $k \in \{0, 1, \ldots, 10\}$. Looking at the Figure 2, it can

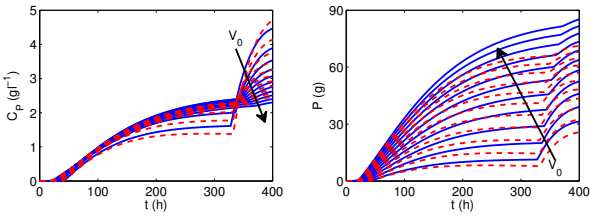

Figure 2. Volume-dependency of C_P and P profiles (CVol - blue full, CVap - red dashed).

be seen that with increasing V_0, product concentration C_P over the cultivation horizon decreases for both of the strategies which can be (once again) explained as the consequence of the inverse proportional effect of the actual volume. On the other hand, the total amount of product P increases with initial volume V_0 increase. This is due to the fact that the total product amount P is proportional not only to product concentration C_P but also to broth volume, $P = C_P V$. From this point of view, the constant volume strategy is able to obtain better results as the volume is held constant - with the constant vaporization, the volume decreases steadily and thus, the total amount of product at t_{end} is lower than with the CVol strategy.

Yet, another interesting tendency is to be observed from Figure 3 - it is a convergency of input profiles to a high-saturation-valued vector with V_0 increase. From technological point of view, this is caused by the increase of V_0/U_{max} ratio - the higher the volume is, the more feed is needed to keep the whole system developing and the higher the V_0/U_{max} ratio is, the longer a high-saturated input must be applied. In order

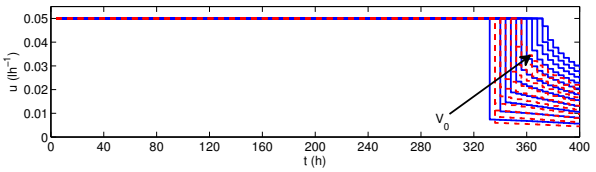

Figure 3. Volume-dependency of input profiles (CVol - blue full, CVap - red dashed).

to inspect the effect of various V_0 in more details, another set of simulations has been performed, however, with a constant ratio $V_0/U_{max} = 7/0.05$. The initial volume V_0 has been set linearly growing as in the previous simulation set. Figure 4

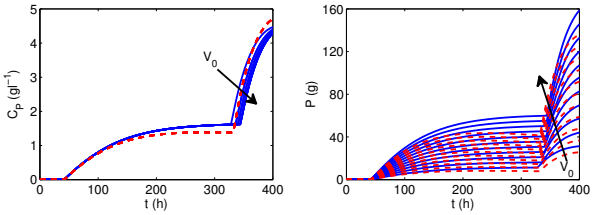

Figure 4. Volume-dependency of C_P and P profiles, fixed V_0/U_{max} ratio (Cvol - blue full, CVap - red dashed).

shows that holding the V_0/U_{max} ratio fixed, C_P profiles aggravation for CVol strategy is not as drastic as in the previous case and, moreover, the C_P profile for CVap strategy does not change at all. However, this is to be expected as with fixed V_0/U_{max} ratio and the same initial concentrations, the system parameters does not change at all and the system with higher V_0 is an exact scale-up of the lower V_0 one. The scale-up claim is supported by the Fig. 5 where input profiles for various V_0 are shown and it is obvious that the dynamical character of the CVap input profile remains the same and the vectors are multiplied by the V_0/U_{max} ratio.

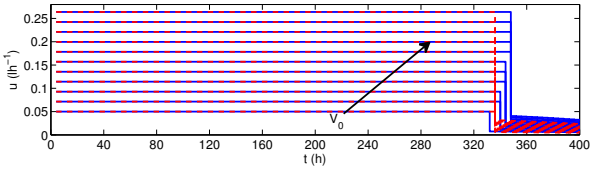

Figure 5. Volume-dependency of input profile, fixed V_0/U_{max} ratio (CVol - blue full, CVap - red dashed).

4.3 Cultivation length dependency

As has already been mentioned, cultivation length is considered to be constant, yet it can be chosen from a set $\{200, 300, 400, 500\}$ h. Figure 6 compares cultivation with classical gradient method (presented in [10]) to the CVol and CVap strategy, respectively. For every chosen cultivation length, it is obvious that the newly proposed strategies achieve better results than the classical one (and the slightly more liberal CVap strategy even more superior) and the product concentrations at the final time $C_P(t_{end})$ are higher with the new strategies.

Looking at the Figure 7, convergence of input profiles to a certain "superprofile" can be seen. Similar kind of convergence has already been mentioned in [9] as well. However, although the profiles are stable backward in time, they do not settle down at the same value (here, we assume settling down in negative march of time). In negative time, CG method settles down on a zero value while CVol and CVap strategies obtained input profiles settle down on upper saturation. The fact that volume is held constant (constantly decreasing, respectively) by the second virtual input (virtual due to the fact that it is not considered in optimization) and it cannot dynamically aggravate the product concentration profile enables to deliver more feed into cultivation tank without negative effect of volume increase and thus, with better fed biomass population, the product concentrations obtained at the end of the cultivation are higher.

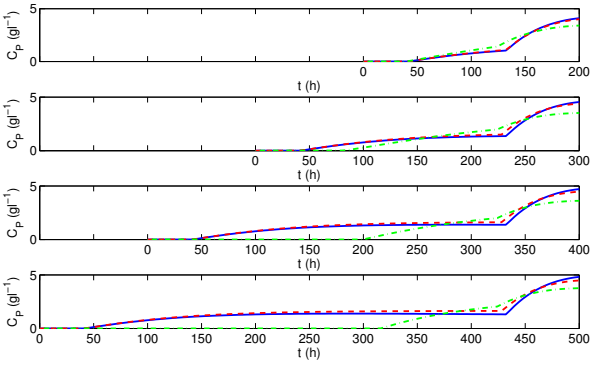

Figure 6. C_P profiles for various cultivation lengths, comparison (CG - green dashdot, CVol - red dashed, CVap - blue full).

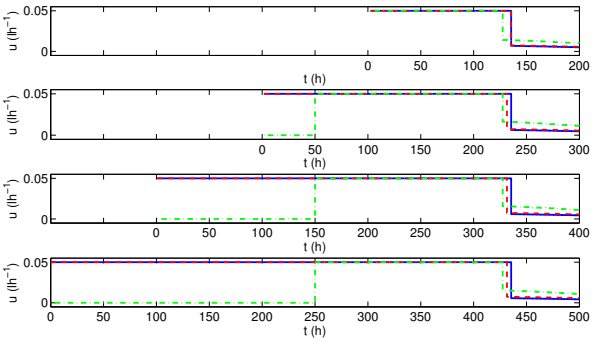

Figure 7. Input profiles for various cultivation lengths, comparison (CG - green dashdot, CVol - red dashed, CVap - blue full).

5 Conclusion

This paper follows the patterns suggested in [10] - a new model of the controlled system involving the second input variable is derived, a successful problem reduction to a single-input optimization is suggested and thanks to this, fresh constant volume and constant vaporization control strategies are introduced. The necessary model adaptation is performed so that it comports with the strategies requirements. Results of the optimization routines are verified on a set of numerical experiments and they are compared to those of previously introduced classical gradient method. The comparison obtained by verifying the newly proposed strategies on a set of numerical simulations and confronting them with the previously introduced classical method can be summarized as a very encouraging - the new strategies achieve better results than the old one, the less conservative constant vaporization strategy shows even slightly more superior performance. Moreover, as one of the former states (volume V) is required to be a parameter in the case of constant volume strategy, result dependencies on this parameter are examined and discussed. A "superprofile" convergence (observed in earlier publications) occurs in this case as well and this supports the claim that it is a property of the optimization issues where the fixed time, fixed initial condition and free terminal condition are considered.

References

[1] S. Lee, "High cell-density culture of Escherichia coli," *Trends in biotechnology*, vol. 14, no. 3, pp. 98–105, 1996.

[2] M. Gregory and C. Turner, "Open-loop control of specific growth rate in fed-batch cultures of recombinant E. coli," *Biotechnology Techniques*, vol. 7, no. 12, pp. 889–894, 1993.

[3] T. Suzuki, T. Yamane, and S. Shimizu, "Phenomenological background and some preliminary trials of automated substrate supply in pH-stat modal fed-batch culture using a setpoint of high limit," *Journal of Fermentation and Bioengineering*, vol. 69, no. 5, pp. 292–297, 1990.

[4] T. Siimes, P. Linko, C. von Numers, M. Nakajima, and I. Endo, "Real-time fuzzy-knowledge-based control of Baker's yeast production," *Biotechnology and bioengineering*, vol. 45, no. 2, pp. 135–143, 1995.

[5] J. Horiuchi, "Fuzzy modeling and control of biological processes," *Journal of bioscience and bioengineering*, vol. 94, no. 6, pp. 574–578, 2002.

[6] A. Ashoori, B. Moshiri, A. Khaki-Sedigh, and M. Bakhtiari, "Optimal control of a nonlinear fed-batch fermentation process using model predictive approach," *Journal of Process Control*, vol. 19, no. 7, pp. 1162–1173, 2009.

[7] Y. Dai and Y. Yuan, "A nonlinear conjugate gradient method with a strong global convergence property," *SIAM Journal on Optimization*, vol. 10, no. 1, pp. 177–182, 2000.

[8] E. Birgin and J. Martínez, "A spectral conjugate gradient method for unconstrained optimization," *Applied Mathematics and optimization*, vol. 43, no. 2, pp. 117–128, 2001.

[9] S. Celikovsky, S. Papacek, A. Cervantes-Herrera, and J. Ruiz-Leon, "Singular perturbation based solution to optimal microalgal growth problem and its infinite time horizon analysis," *Automatic Control, IEEE Transactions on*, vol. 55, no. 3, pp. 767–772, 2010.

[10] M. Pčolka and S. Čelikovský, "Gradient Method Optimization of Penicillin Production," in *Chinese Control and Decission Conference*, 2012 (accepted).

[11] J. Van Impe and G. Bastin, "Optimal adaptive control of fed-batch fermentation processes with multiple substrates," in *Control Applications, 1993., Second IEEE Conference on*. IEEE, 2002, pp. 469–474.

[12] A. Constantinides, J. Spencer, and E. Gaden Jr, "Optimization of batch fermentation processes. II. Optimum temperature profiles for batch penicillin fermentations," *Biotechnology and Bioengineering*, vol. 12, no. 6, pp. 1081–1098, 1970.

[13] D. Contois, "Kinetics of bacterial growth: relationship between population density and specific growth rate of continuous cultures," *Microbiology*, vol. 21, no. 1, p. 40, 1959.

[14] G. Briggs and J. Haldane, "A note on the kinetics of enzyme action," *Biochemical journal*, vol. 19, no. 2, p. 338, 1925.

[15] A. Bryson and Y. Ho, "Applied optimal control," *New York: Blaisdell*, 1969.